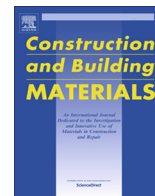




Contents lists available at ScienceDirect

Construction and Building Materials

journal homepage: www.elsevier.com/locate/conbuildmat

Behavior of hollow steel sections strengthened with CFRP

Anwar Badawy Badawy Abu-Sena^a, Mohamed Said^{a,*}, M.A. Zaki^b, Mohamed Dokmak^b^a Faculty of Engineering (Shoubra), Benha University, Egypt^b Housing and Building National Research Center, Egypt

H I G H L I G H T S

- Study of short SHS and RHS steel columns strengthened with CFRP.
- CFRP delays the elastic local buckling and increases the column axial capacity.
- The full strengthening of HSS delays the local buckling occurrence.
- The partial strengthening of HSS is significantly affected by spacing between strips.
- Non-linear finite element analyses were performed and assessed with experimental results.

A R T I C L E I N F O

Article history:

Received 7 October 2018

Received in revised form 16 December 2018

Accepted 31 January 2019

Keywords:

Local buckling
Hollow steel sections (HSS)
Strengthening
CFRP

A B S T R A C T

Experimental and numerical investigations have been performed on twenty short square and rectangular hollow sections (SHS and RHS) steel columns. The confinement action provided by the CFRP wrapping effectively delays the local buckling of fully strengthened specimens. However, in case of partially strengthened specimens, failure occurs at the non-strengthened zones between CFRP strips. The enhancement in ultimate capacity ranges between 19.1% and 34.5% for SHS, and between 18% and 41.3% for RHS specimens. It has been noticed that, the improvement in the behavior for specimens strengthened with two layer strips is limited compared to specimens strengthened with one layer strips. The finite element results are found to be in good agreement with their experimental counterparts. The reliability index between the finite element and the experimental ultimate capacities ranges between 0.01 and 0.1. An analytical model has been developed to predict the failure load of the control specimens.

© 2019 Elsevier Ltd. All rights reserved.

1. Introduction

Hollow steel sections (HSS) are commonly utilized in steel structures for their high strength-to-weight ratios. They are an assemblage of single thin plate elements connected together to shape the desired section. Members of thin walled sections may buckle locally at a stress level lower than the yield point of steel when they are subjected to axial compression [1]. This premature failure is unacceptable specifically when HSS are used as main members in vital structures such as bridges. Square hollow section (SHS) and rectangular hollow section (RHS) columns are locally buckled with inward and out ward deformations at their section. These deformations are repeated with a successive sine wave along column longitudinal axis [2].

External strengthening of HSS has gone through many stages starting from using steel plates, which might be either bolted or

welded to the premier structure, till applying fiber reinforced polymer (FRP) materials. Many drawbacks have faced strengthening using steel plates. Adding a considerable dead load to strengthened elements and fatigue problems associated with welding process are samples of these obstacles [3].

Several laboratory studies have shown that CFRP plates can be used to effectively strengthen steel bridge girders [4]. A reasoned review on research works covering the efficiency of FRP strengthening systems on metallic structures was presented by Zerbo et al. [5] This review concluded that; the strengthening performance using FRP mainly depends on the bond between FRP fabrics and strengthened steel elements. Zhao and Zhang [6] presented a review on research works such as the strengthening of HSS members, bond between steel and FRP, and fatigue crack propagation in the FRP–Steel system.

An experimental program associated with analytical and numerical investigations were presented by Colombi and Poggi [7]. They aimed at studying the behavior of steel beams strengthened by CFRP strips. The ultimate load carrying capacity was increased by about 40% when two layers of CFRP strips were

* Corresponding author.

E-mail addresses: badawy@feng.bu.edu.eg (A.B.B. Abu-Sena), Mohamed.abdelgaffar@feng.bu.edu.eg (M. Said).

attached to the tension flanges. Narmashiri et al. [8] studied different failure patterns of CFRP flexural strengthened steel I-beams. Ghafoori et al. [9], Yu et al. [10] and Kamruzzaman et al. [11], discussed the utilization of FRP reinforcing techniques to prevent structural steel elements from fatigue damage.

Shaah and Fam [12] retrofitted short and long HSS columns with CFRP sheets. Effects of number of layers and fiber orientations were investigated for two types of CFRP sheets. Maximum enhancement of about 18% and 23% in load carrying capacity was achieved for short and long columns respectively. The utmost gain was achieved for specimens with three layers applied on four sides. The axial capacity of strengthened long columns was estimated based on the design equation of the Canadian Standards Association [13].

Bambach et al. [14] showed that the application of CFRP to short axially compressed cold formed SHS may provide increases in axial capacity up to two times of the non-strengthened steel column. Sundarraja et al. [15] experimentally and numerically investigated the behavior of axially compressed HSS columns strengthened by CFRP strips with different spacing and number of layers. The ultimate strength enhanced with the application of CFRP strips with percentage up to 44% more than the control specimen.

Ghaemdoust et al. [16] utilized experimental test and numerical simulation to study the retrofitting of box shaped axially compressed members with initial deficiency using CFRP sheets. The ultimate load has been increased by about 55% due to applying the CFRP. Haedir and Zhao [17] presented the experimental and numerical evaluations of the effect of external strengthening of circular short columns using (CFRP) sheets. The experimental results indicated that, the axial compression capacity of columns increases with increasing the number of CFRP layers. Sundarraja and Shanmugavalli [18] presented a feasibility research aiming at predicting the suitable wrapping scheme of FRP to enhance the structural behavior of circular hollow steel (CHS) sections. The fully wrapped specimens with two layers of CFRP sheets had the greatest enhancement in axial capacity.

For columns of opened sections, Kalavagunta et al. [19] revealed a design method based on British Standards [20] to predict the load carrying capacity of strengthened cold formed steel channel section strengthened by CFRP fabrics. It was found that; the strength

of CFRP strengthened steel columns gained an increase up to 10% greater than the plain cold formed steel sections.

Recently, Amoush and Ghanem [21] carried out an experimental study on twelve controls, partially and fully strengthened cold formed lipped channel columns with different parameters. They utilized the finite element method as a numerical tool, to simulate the laboratory results. The behavior and capacities of the partially and the fully strengthened columns were improved with applying the proposed strengthening technique.

Shahraki et al. [22] studied the effect of strengthening of axially loaded deficient SHS columns using CFRP and steel plates. They performed experimental and numerical investigations on fourteen specimens of different parameters. The carrying capacity and failure pattern were improved at strengthened specimens compared to control specimens. It was founded that; utilizing CFRP sheets is more effective than welding steel plates to retrofit deficient SHS columns.

Karimian et al. [23] and Shahabi and Narmashiri [24] studied the effect of retrofitting deficient CHS columns of various deficient locations using CFRP. They concluded that; utilizing CFRP sheets compensates the reduction in capacity of deficient columns and control the local deformation around the deficiency zone.

The current study aims at investigating the effect of CFRP in controlling local buckling in-stability mode to increase the ultimate capacity of axially compressed SHS and RHS short columns. This study presents the strength and structural behavior of SHS and RHS strengthened with CFRP utilizing three different techniques. The first technique is the full wrapping, the second is using strips of single layers and the third is using strips with two layers. The results of experimental work performed in this research will be verified using the finite element non-linear analysis as a numerical tool in addition to using a developed analytical model.

2. Experimental program

Twenty specimens are tested to study the local buckling behavior of SHS and RHS short columns wrapped with CFRP under pure compression. Five assemblies of commercially available SHS and RHS are chosen carefully with plate slenderness which guarantees that local buckling is the governing failure mode. For short col-

Table 1
Studied SHS and RHS with the applied strengthening technique.

Sec. Type	Section	Sectional dimensions (mm)			Plate Slenderness ratios		Specimen ID	Strengthening scheme	
		Width (b)	Depth (d)	Thickness (t)	b/t	d/t			
SHS	S-100 × 100 × 1.5	100.0	100.0	1.5	67.0	67.0	S-10-C	Non-strengthened	
							S-10-FF	Full wrapped	
							S-10-FS1L	Strips of one layer	
	S-80 × 80 × 1.5	80.0	80.0	1.5	53.0	53.0	S-10-FS2L	Strips of two layers	
							S-8-C	Non-strengthened	
							S-8-FF	Full wrapped	
	S-70 × 70 × 1.4	70.0	70.0	1.4	50.0	50.0	S-8-FS1L	Strips of one layer	
							S-8-FS2L	Strips of two layers	
							S-7-C	Non-strengthened	
RHS	R-40 × 100 × 1.2	40.0	100.0	1.2	33.0	83.0	S-7-FF	Full wrapped	
							S-7-FS1L	Strips of one layer	
							S-7-FS2L	Strips of two layers	
	R-40 × 80 × 1.1	40.0	80.0	1.1	36.0	73.0	R-4-10-C	Non-strengthened	
							R-4-10-FF	Full wrapped	
							R-4-10-FS1L	Strips of one layer	
								R-4-10-FS2L	Strips of two layers
								R-4-8-C	Non-strengthened
								R-4-8-FF	Full wrapped
							R-4-8-FS1L	Strips of one layer	
							R-4-8-FS2L	Strips of two layers	

umns, transverse CFRP layers are more effective in confining the outward local buckling than longitudinal confining [12]. For this reason, the chosen wrapping schemes are applied in transverse direction of the studied columns. The parameters for each group with full wrapping and strips systems are shown in Table 1.

2.1. Materials of selected specimens.

A tensile coupon test is performed for each studied section to specify its mechanical characteristics. The representative stress-strain curves of all tested specimens are shown in Fig. 1. Mechanical properties of the tested steel specimens are shown in Table 2.

A unidirectional woven carbon fiber fabric SikaWrap®-300c is used for strengthening. It is mid-strength carbon fibers of 0.17 mm thickness and having modulus of elasticity of 230 GPa and tensile strength of 4000 MPa [25]. Sikadur®-330 is used to obtain an adequate bond between steel columns and carbon fiber [26].

2.2. Specimens preparation and test setup

All selected steel specimens (SHS and RHS) have a total length of 700.0 mm. For specimens wrapped with CFRP strips, the clear spacing between strips is 50.0 mm and the width of strips is 100.0 mm. Fig. 2 shows the schemes of wrapping system. Fiber setup process is shown in Fig. 3. After finishing wrapping process of CFRP fabrics, all wrapped specimens are cured at room temperature for more than 7 days according to manufacturer recommendations.

Two column heads of 20 mm thickness are attached to both column ends to ensure a uniform stress distribution to all column sides. Each column head is attached with four angles of standard Euro section 50×5 to avoid web crippling phenomenon at stress concentration zone, in addition, these angles prevent column twisting. The prepared SHS and RHS short columns are tested under axial compression using testing machine of 2000 kN. capacity. The applied load is measured with a 500 kN. capacity load cell. Axial deformation of tested specimen is monitored using linear voltage displacement transducer (LVDT). One 6 mm electric resistance strain gauge (S.S.G) is directly attached to steel in longitudinal direction at the anticipated locations of local buckling to investigate the behavior of steel. Two 10 mm electric resistance strain gauges (F.S.G) are fastened over carbon fibers transversally to measure fiber strain at max stressed zone where local buckling is expected to occur Fig. 4 shows test setup and the attached instruments. Columns are subjected to axial compression load with small increments till failure. Failure behavior accompanying to ultimate load was noticed for each specimen.

3. Test results

3.1. Ultimate capacity and axial deformation

The axial load-displacement curves of the studied specimens are presented in Figs. 5–9. These figures illustrate the behavior of specimens during the loading and show the effect of strengthening on the ultimate capacities and axial deformations of the studied specimens.

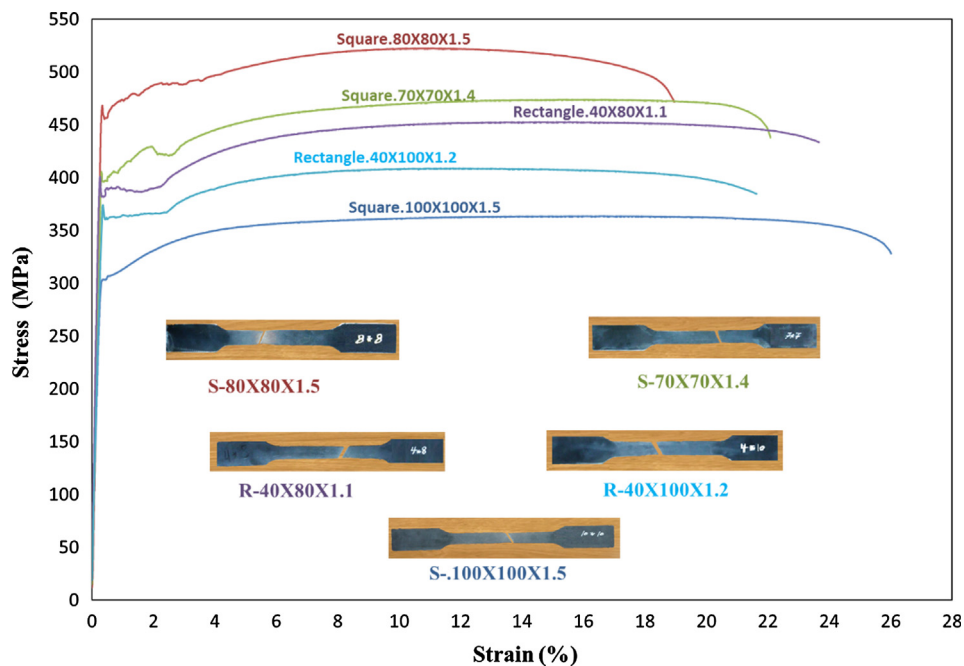


Fig. 1. Stress-strain curves of tested steel specimens.

Table 2
Mechanical properties of studied steel sections.

Specimen Section	Section area (mm ²)	Modulus of Elasticity (GPa)	Yield strength (MPa)	Ultimate strength (MPa)
S-100 × 100 × 1.5	591.0	178.0	303.0	364.0
S-80 × 80 × 1.5	471.0	172.0	456.0	522.0
S-70 × 70 × 1.4	384.0	178.0	397.0	474.0
R-40 × 100 × 1.2	330.0	186.0	360.0	409.0
R-40 × 80 × 1.1	259.0	186.0	385.0	452.0

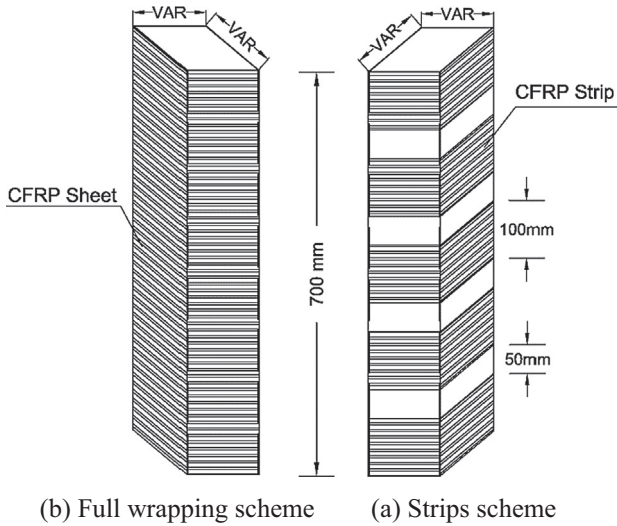


Fig. 2. Hollow steel sections wrapping schemes.



(a) Full strengthened specimen (b) Partial strengthened specimen

Fig. 3. CFRP wrapping process.

From Fig. 5, it can be noticed that, a significant enhancement in axial load capacity is achieved with full wrapping of the section $S-100 \times 100 \times 1.5$. The ultimate axial load for fully wrapped column increases by about 30.2%. Whereas, the enhancement in the ultimate capacity for specimens strengthened with fiber strips (one and two layers) is about 20.9% and 19.1% respectively. A considerable decrease in axial shortening of about 32.1%, 21.7% and 15.1% is also observed for the fully wrapped, single layer and double layers strips respectively.

A similar behavior can be noticed from Figs. 6 and 7 for sections $80 \times 80 \times 1.5$ and $70 \times 70 \times 1.4$ respectively. The increase in the ultimate load is about 27.7% and 34.5% for fully wrapped specimens S-8-FF and S-7-FF, whereas the reduction in the axial deformation is about 9.2% and 15.7% respectively. The utmost increase in the ultimate capacity load for specimens strengthened with fiber strips is about 26.3% for specimen S-8-FS2L. Figs. 5–7, demonstrate that the axial stiffness generally increases by applying any of the three proposed schemes.

On the other hand, the ultimate load for RHS provided with CFRP is increased as shown in Figs. 8 and 9. The increase in the ultimate load is about 41.3% and 18% for the fully wrapped specimens R4-8-FF and R-4-10-FF respectively. The maximum increase in ultimate

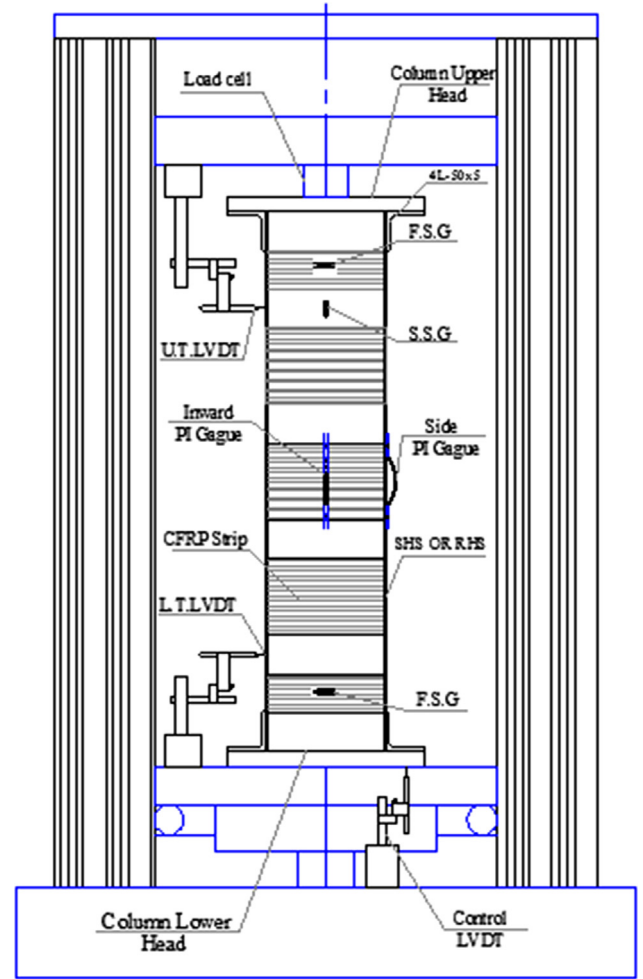


Fig. 4. Schematic details of the test setup.

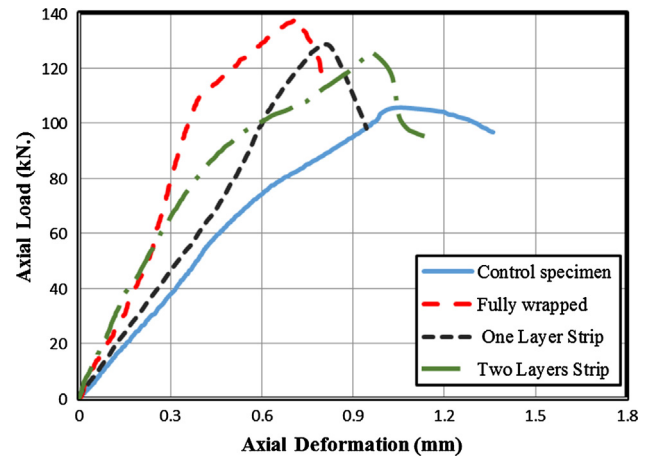


Fig. 5. Load-deformation curves for SHS short columns of sec. $100 \times 100 \times 1.5$.

load for partially strengthened RHS columns is about 31.0% for R-4-10-FS2L.

Comparison of results shows that, the largest effect of CFRP on the ultimate load and stiffness is attained at the full wrapping system. The results reveal a decline in the axial deformation for specimens strengthened with CFRP. Failure loads and corresponding axial shortening for all specimens are summarized in Table 3.

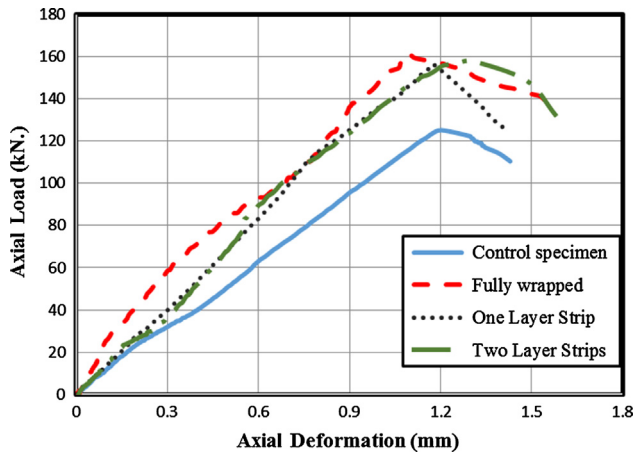


Fig. 6. Load-deformation curves for SHS short columns of sec.80 × 80 × 1.5.

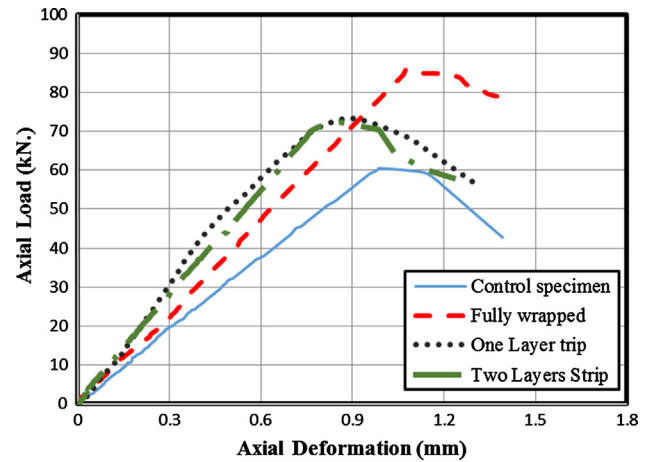


Fig. 9. Load-deformation curves for RHS short columns of sec.40 × 80 × 1.1.

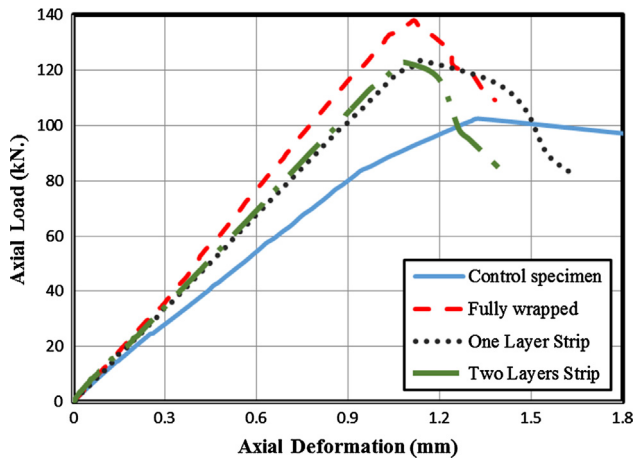


Fig. 7. Load-deformation curves for SHS short columns of sec.70 × 70 × 1.4.

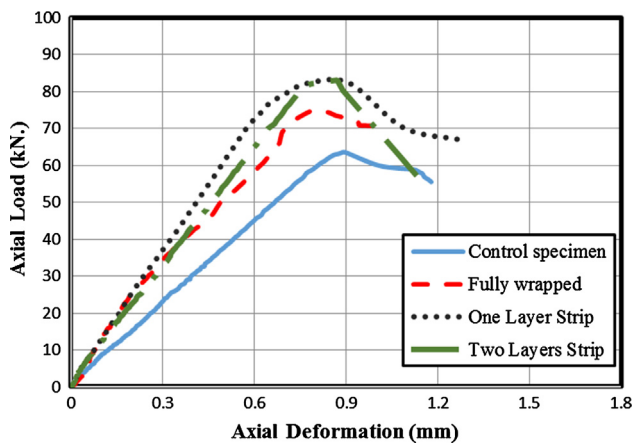


Fig. 8. Axial load-deformation curves for RHS short columns of sec.40 × 100 × 1.2.

Shaat and Fam [12] experimental investigation showed an increase of 15% for fully strengthened SHS with single transverse layer of CFRP while the capacity of column increased by 18% when strengthened by two layers of CFRP. Experimental and numerical investigations conducted by Sundararaja et al. [15] on partially strengthened SHS columns showed an increase in axial capacity reached to 32.8% of strengthened columns with one layer strips.

The increase in spacing between strips led to the decrease in axial capacity.

All tested specimens failed due to post-local buckling phenomenon without any remarkable local failure neither in CFRP sheets nor in adhesion between steel and CFRP. Table 4 shows the monitored strain at failure for both steel and fiber sheets.

All specimens failed before the yielding of steel as shown in Table 4 Accordingly; the tested columns failed at elastic zone of steel after occurrence of elastic local buckling. The obtained fiber strain results are lower than the nominal fiber strain CFRP (0.015) as recommended by the manufacturer technical data sheet [25]. Fiber laminates did not reach their nominal capacity that illustrates the observed non-fracture occurrence in fiber laminates till failure of wrapped specimens

3.2. Failure modes

The non-strengthened control columns are locally buckled, where two opposite sides buckled outward and the other two sides buckled inward, as shown in Fig. 10a. The fully wrapped specimens fail in a similar manner, with two sides buckling outward, and the other two sides inward. However, the confinement produced by wrapped CFRP layers plays a considerable role in delaying buckling occurrence, which results in increasing column axial capacity (Fig. 10b).

For partially strengthened columns using CFRP with one-layer or two-layer strips, the non-strengthened steel zone is buckled between two alternate fiber strips as shown in Fig. 10c and d. The presence of CFRP strips prevents the successive buckling waves along column height which, causes the delay of buckling occurrence but not similar to full wrapping effect. The enhancement percentages may be increased much more by increasing strip width or decreasing strips interval distance or both. Limited improvement is noticed for specimens with two layers strips compared to specimens with one layer strips.

In the same manner, the axial capacity of rectangle columns is enhanced when fully and partially strengthened by CFRP. The increase of ultimate load for the R-4-10-FF section is about 18%, while R-4-8-FF section has an increase of 41.3%. To understand the reason of the inordinate difference between the R-4-10-FF and R-4-8-FF sections, the deformed shape of the two specimens were thoroughly studied. It has been noticed that, the failure of specimen R-4-10-FF was due to inward buckling of the large plates as shown in Fig. 11a, while, the outward buckling was the governing failure for specimen R-4-8-FF as shown in Fig. 11b. The inward buckling at large plates of the rectangle specimen causes large

Table 3
Ultimate capacity and axial shortening at failure of tested columns.

Section	Specimen	Ultimate Compressive Load (kN.)	Axial Capacity Increase (%)	Axial Deformation at Failure (mm)
Square 100 × 100 × 1.5	S-10-C	105.8	---	1.06
	S-10-FF	137.7	30.2	0.72
	S-10-FS1L	127.9	20.9	0.83
	S-10-FS2L	125.96	19.1	0.9
Square 80 × 80 × 1.5	S-8-C	125.1	---	1.2
	S-8-FF	161.8	29.3	1.09
	S-8-FS1L	156.3	24.9	1.18
	S-8-FS2L	158	26.3	1.3
Square 70 × 70 × 1.4	S-7-C	102.6	---	1.33
	S-7-FF	138	34.5	1.12
	S-7-FS1L	123.4	20.3	1.14
	S-7-FS2L	123.115	20.0	1.08
Rectangular 40 × 100 × 1.2	R-4-10-C	63.5	---	1.01
	R-4-10-FF	74.9	18.0	0.79
	R-4-10-FS1L	82.3	29.6	0.91
	R-4-10-FS2L	83.2	31.0	0.87
Rectangular 40 × 80 × 1.1	R-4-8-C	60.63	---	0.99
	R-4-8-FF	85.7	41.3	1.08
	R-4-8-FS1L	73.4	21.1	0.91
	R-4-8-FS2L	72.4	19.4	0.86

Table 4
Strain of steel and fiber at failure of tested specimens.

Group	Specimen	Steel axial strain		CFRP strain at failure
		strain at failure	yielding strain (coupon test)	
A	S-10-C	0.0012	0.0022	
	S-10-FF	0.0016		0.0014
	S-10-FS1L	0.0014		0.0007
	S-10-FS2L	0.0014		0.0011
B	S-8-C	0.0015	0.0032	
	S-8-FF	0.0017		0.0009
	S-8-FS1L	0.0019		0.0001
	S-8-FS2L	0.0020		0.0003
C	S-7-C	0.0016	0.0025	
	S-7-FF	0.0019		0.003
	S-7-FS1L	0.0014		0.0007
	S-7-FS2L	0.0015		0.0007
D	R-4-8-C	0.0014	0.0026	
	R-4-8-FF	0.0018		0.0020
	R-4-8-FS1L	0.0016		0.0016
	R-4-8-FS2L	0.0016		0.0003
E	R-4-10-C	0.0011	0.0024	
	R-4-10-FF	0.0013		0.0004
	R-4-10-FS1L	0.0014		0.001
	R-4-10-FS2L	0.0016		0.002

stresses at interface layer between steel and fiber, which results in fiber de-lamination that in turn reduces the stiffness of column resulting in an early failure.

The difference in failure mode between the two rectangular sections is expected to be due to the presence of different initial imperfection. So, the enhancement value of 41.3% at R-4-8-FF cannot be considered as a reference value, because the inward buckling may govern the failure of some other sections leading to reduced strength enhancement as in the case of R-4-10-FF section.

For partially wrapped rectangular specimens, a noticed enhancement in capacity is achieved. Similar to square double layer strengthened columns, a limited additional increase in capacity is achieved when using two layers strips instead of one layer strips.

4. Finite element modeling

Nonlinear buckling analysis using ANSYS.15.0 is utilized to illustrate the effect of CFRP confinement upon HSS local buckling mode and the ultimate failure load as well. The thickness of steel

tubes is taken according to Table 1, while; the CFRP sheets thickness is taken equal to 1 mm for single layer.

The material of steel is simulated using bilinear stress-strain curve as the current study is bounded at the elastic buckling zone. Therefore; the curve of steel is drawn by specifying Young's modulus and yielding strength (Table 2). The Poisson's ratio is taken equal to 0.3.

CFRP material is modeled as orthotropic unidirectional material. The CFRP laminate including the carbon fiber and the resin is defined by linear stress-strain curve [14]. The mechanical properties as per the manufacturer specifications [25] are; $F_y = 3200$ MPa and $E = 220$ GPa. The Poisson's ratio of CFRP is taken equal to 0.22 [15].

Thin shell element (SHELL181) is used to simulate steel columns. SHELL181 is suitable for analyzing thin to moderately-thick shell structures. However, structural solid element SOLID185 is used to represent the applied CFRP as modeled by Sundarraja, et al [15]. The contact between steel section and carbon fiber sheets or strips is provided by the contact element (CONTA174). CONTA174 is used to represent contact and sliding between tar-

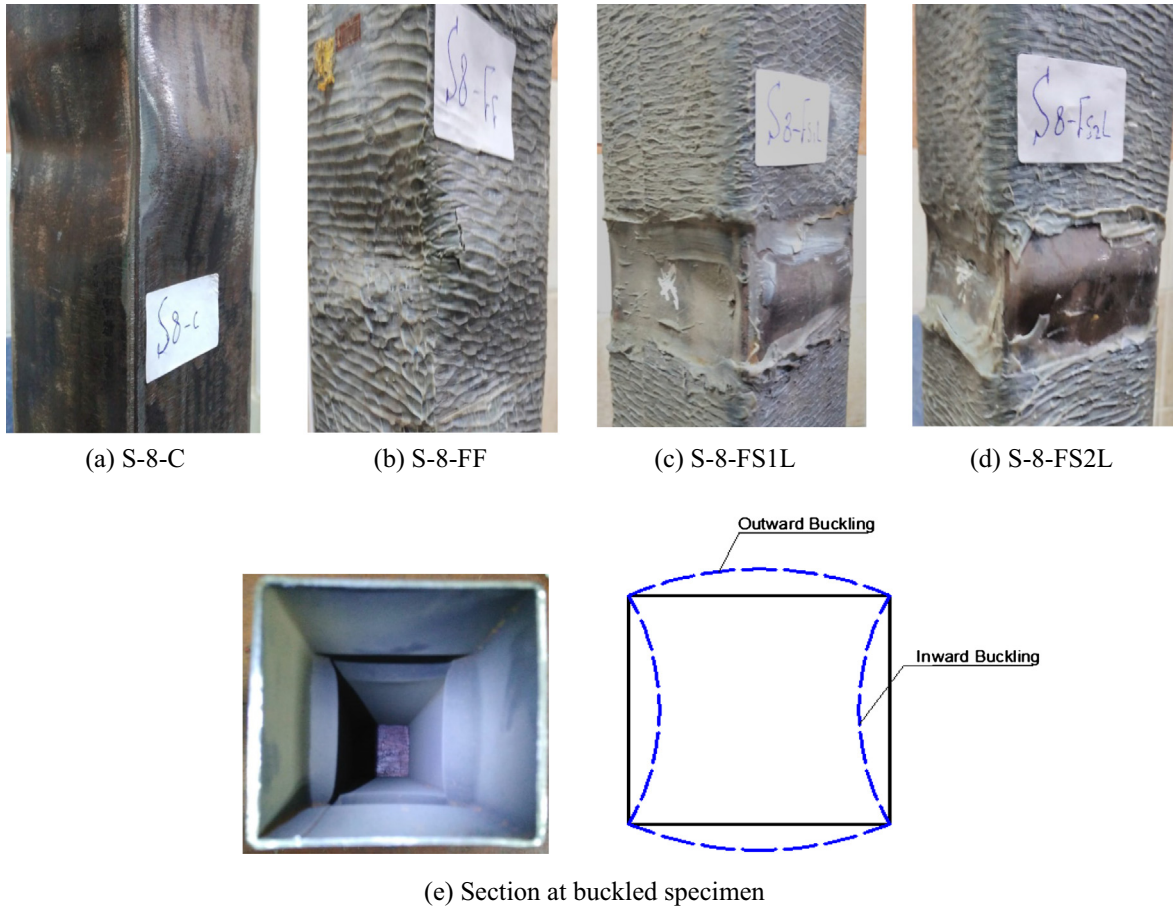


Fig. 10. Failure modes of section (S-80x80x1.5): a) Control specimen, b) Fully wrapped, c) Single layer strips, d) Double layers strips and e) Buckled cross section.

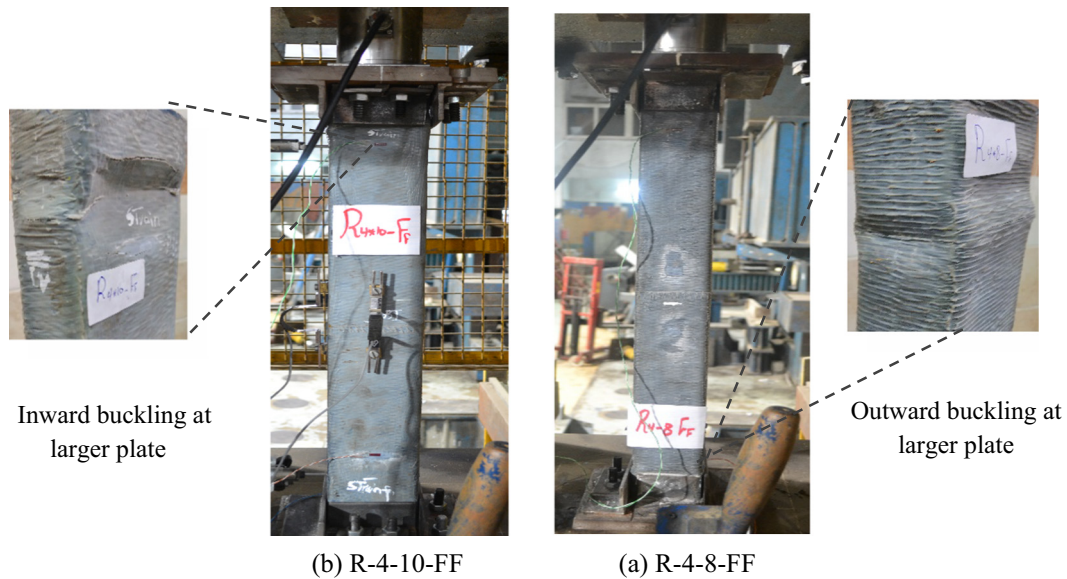


Fig. 11. Failure at full strengthened RHS columns.

get surfaces and a deformable surface. The behavior of contact surface is chosen to be bonded. The separation between bonded surfaces is also allowed.

Different mesh sizes for steel specimen model have been tried till achieving the optimum size with dimension of

10 mm × 10 mm. Carbon sheets was discretized at the transverse direction only with the same size to represent the unidirectional behavior of CFRP element.

All specimens are restrained laterally at both upper and lower end nodes, thus the specimen is prevented from rotation and lat-

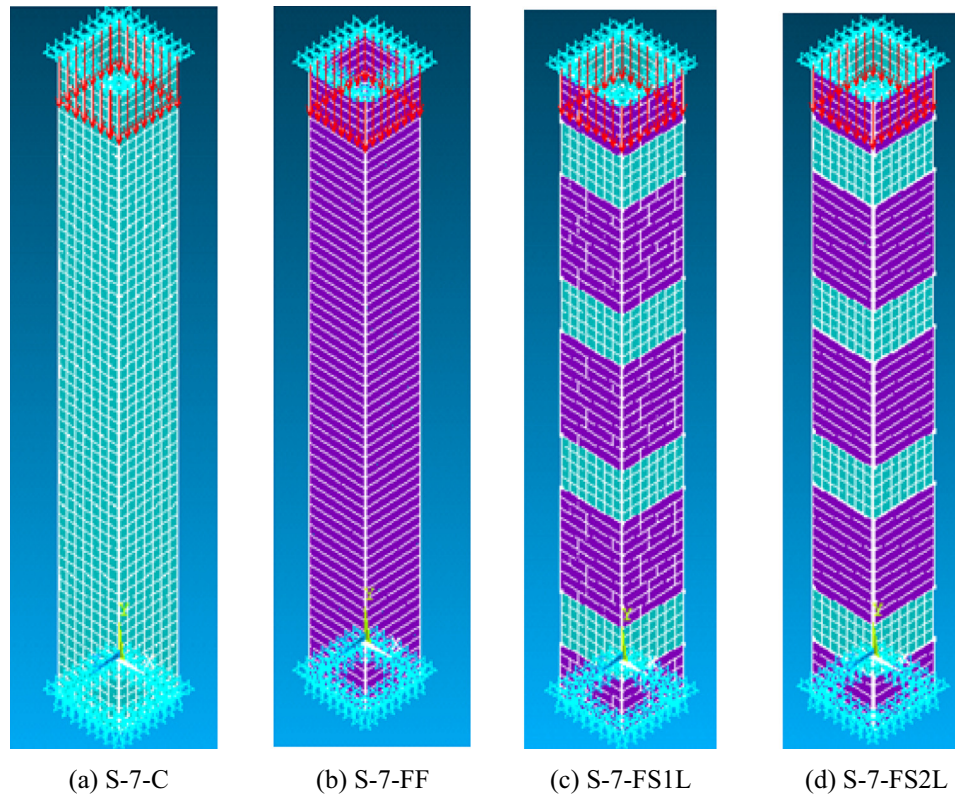


Fig. 12. Created models for section S-70 × 70 × 1.4: a) Control specimen, b) Fully wrapped, c) Single layer -strips, and d) Double layer- strips.

eral translation at the two ends. Axial load is applied to the top nodes of column while axial restraints in direction opposing to loading are assigned to the bottom nodes of column. Fig. 12 shows the finite element mesh, the boundary conditions and the arrangement of CFRP layers for different confining systems for section S-70 × 70 × 1.4 as an example.

Geometrical imperfection can be implemented by applying either small lateral load, or small initial deformation to the initial geometry. In this research, initial deformation is used as

initial imperfection. The critical Eigen value mode is used to apply this small geometry perturbation using ANSYS-UPGEOM command.

Analysis method called the arc length control method is used to control load application to avoid numerical instability occurrence using the common (load control method). Using this method, points corresponding to consecutive load increments are evenly spaced along the load-displacement curve, which itself is constructed during load application (Pietropaoli and Riccio [27]).

Table 5
Comparison between Experimental and Finite Element Ultimate Capacities.

Section	Specimen	Ultimate Compressive Load (KN.)		Axial Capacity Increase (%)		Exp./F. E.
		Exp.	F. E.	Exp.	F. E.	
Square 100 × 100 × 1.5	S-10-C	105.8	107	----	----	0.99
	S-10-FF	137.7	145.8	30.2	36.26	0.94
	S-10-FS1L	127.9	136.6	20.9	27.66	0.94
	S-10-FS2L	125.96	140.2	19.1	31.03	0.90
Square 80 × 80 × 1.5	S-8-C	125.1	129.7	----	----	0.96
	S-8-FF	161.8	172	29.3	32.61	0.94
	S-8-FS1L	156.3	160.1	24.9	23.44	0.98
	S-8-FS2L	158	159.2	26.3	22.74	0.99
Square 70 × 70 × 1.4	S-7-C	102.6	104.93	----	----	0.98
	S-7-FF	138	138.2	34.5	31.71	1.00
	S-7-FS1L	123.4	125.3	20.3	19.33	0.98
	S-7-FS2L	123.115	124.2	20.0	18.29	0.99
Rectangular 40 × 100 × 1.2	R-4-10-C	63.5	66.93	----	----	0.95
	R-4-10-FF	74.9	71.5	18.0	6.82	1.05
	R-4-10-FS1L	82.3	87.7	29.6	32.68	0.94
	R-4-10-FS2L	83.2	87.8	31.0	32.83	0.95
Rectangular 40 × 80 × 1.1	R-4-8-C	60.63	61.8	----	----	0.98
	R-4-8-FF	85.7	87.7	41.3	41.91	0.98
	R-4-8-FS1L	73.4	78.8	21.1	27.51	0.93
	R-4-8-FS2L	72.4	78.2	19.4	26.54	0.93

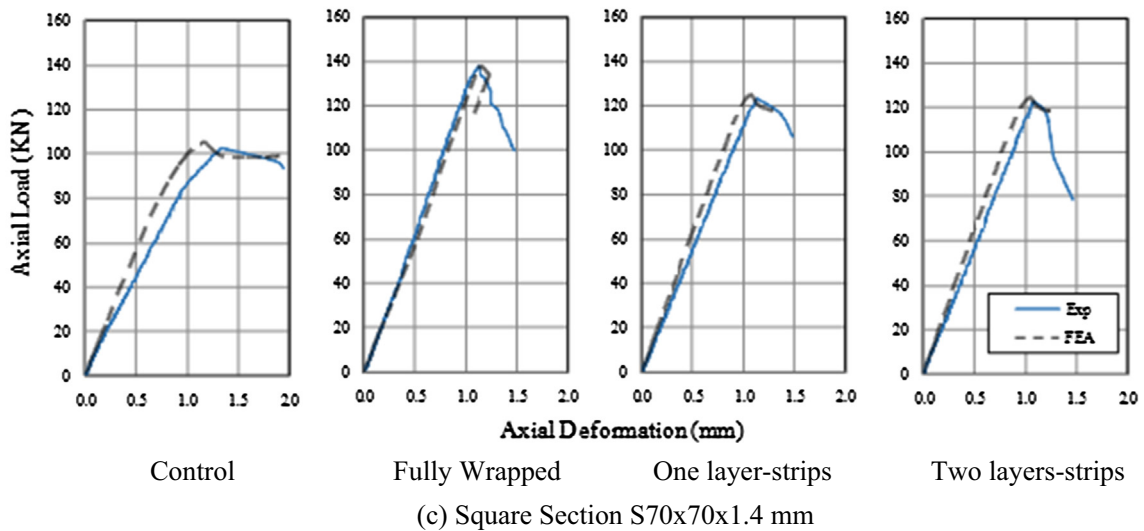
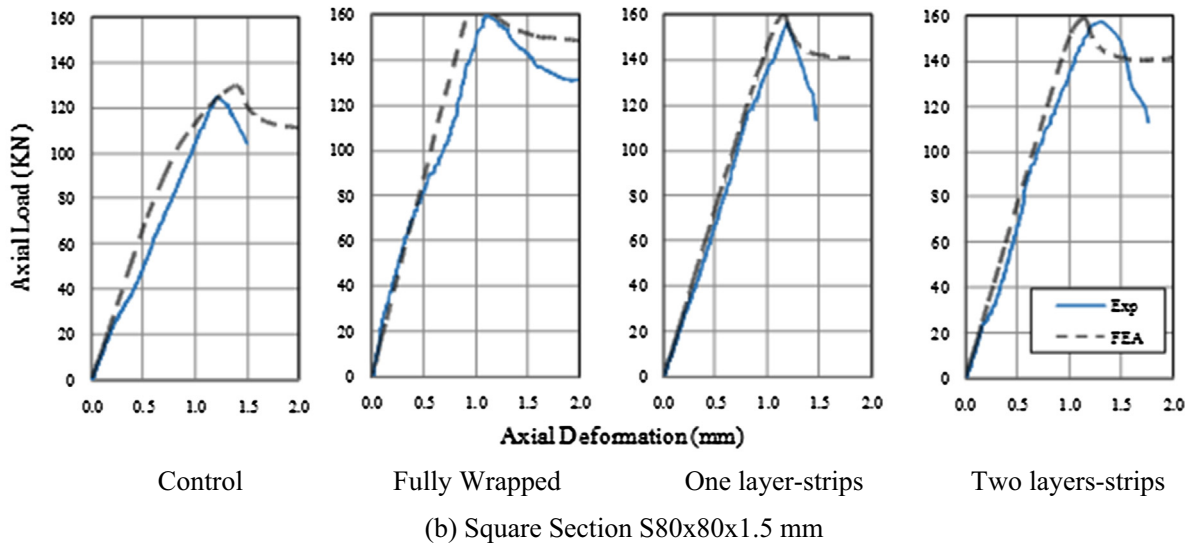
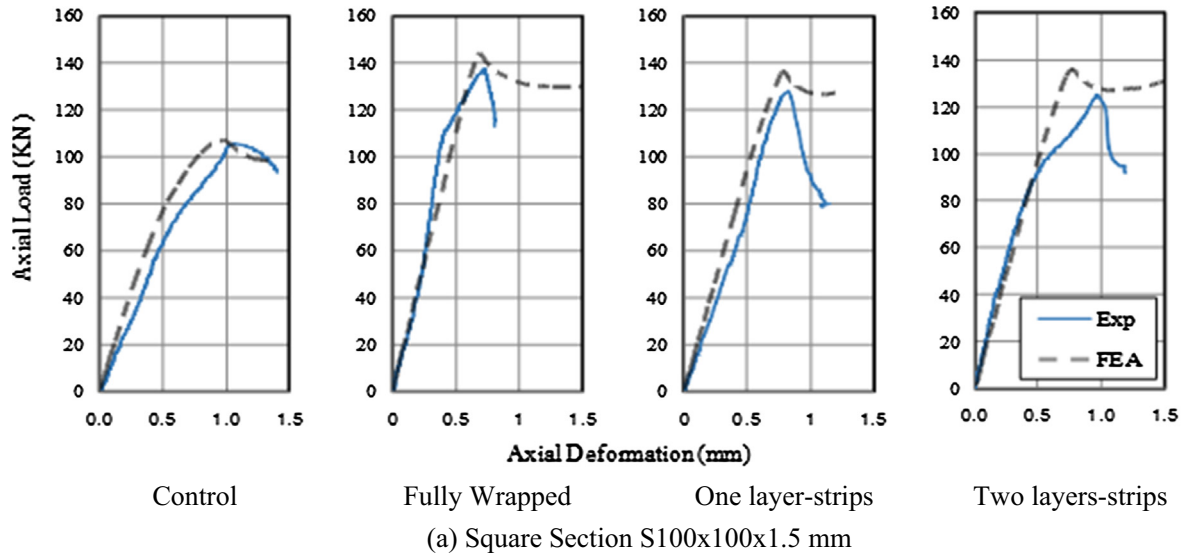


Fig. 13. Comparison between experimental and analytical load-deformation relations, for the studied SHS short columns.

4.1. Axial capacity and deformation

The ultimate axial load of each specimen obtained from both experiments and finite element modeling are presented in Table 5. It can be noticed that, the ratio of experimental to the finite element ultimate capacity for the all columns ranges between 0.90 and 1.05.

Figs. 13 and 14 present a comparison between the load-shortening curves obtained from the tests and finite element analyses for the SHS and RHS respectively. It can be concluded that, strengthening of closed SHS and RHS columns by full wrapping technique using CFRP sheets leads to an increase in stiffness and also provides an enhancement in axial capacity. The partial strengthening technique provides a moderate increase in stiffness and axial capacity.

4.2. Failure modes

Fig. 15 shows the failure mode of a representative control SHS column of section S-70 × 70 × 1.4 obtained from both experimental work and the finite element analysis.

In case of fully wrapped specimens, the confining action presented by CFRP wrapping plays an important role in improving columns cross section behavior against outward deformation. Therefore, the boundary conditions of inward deformed sides are changed from flexible edges to be stiffened edges, as can be noticed from Fig. 16. The failure of fully wrapped S-7-FF column is shown in Fig. 17.

As mentioned before, for partially strengthened columns using one layer and two layers strips, the presence of fiber strips prevents steel buckling at wrapped zones. Buckling half waves are shifted to the un-wrapped zones and that forces the buckling mode to be changed to a higher mode leading to higher failure load. Figs. 18 and 19 show the buckling shapes of S-7-FS1L and S-7-FS2L specimens respectively.

5. Analytical investigation

The box section may be considered as an assemblage of four slender plates with two simply supported short edges, and two elastically restrained long edges. Accordingly, the boundary condi-

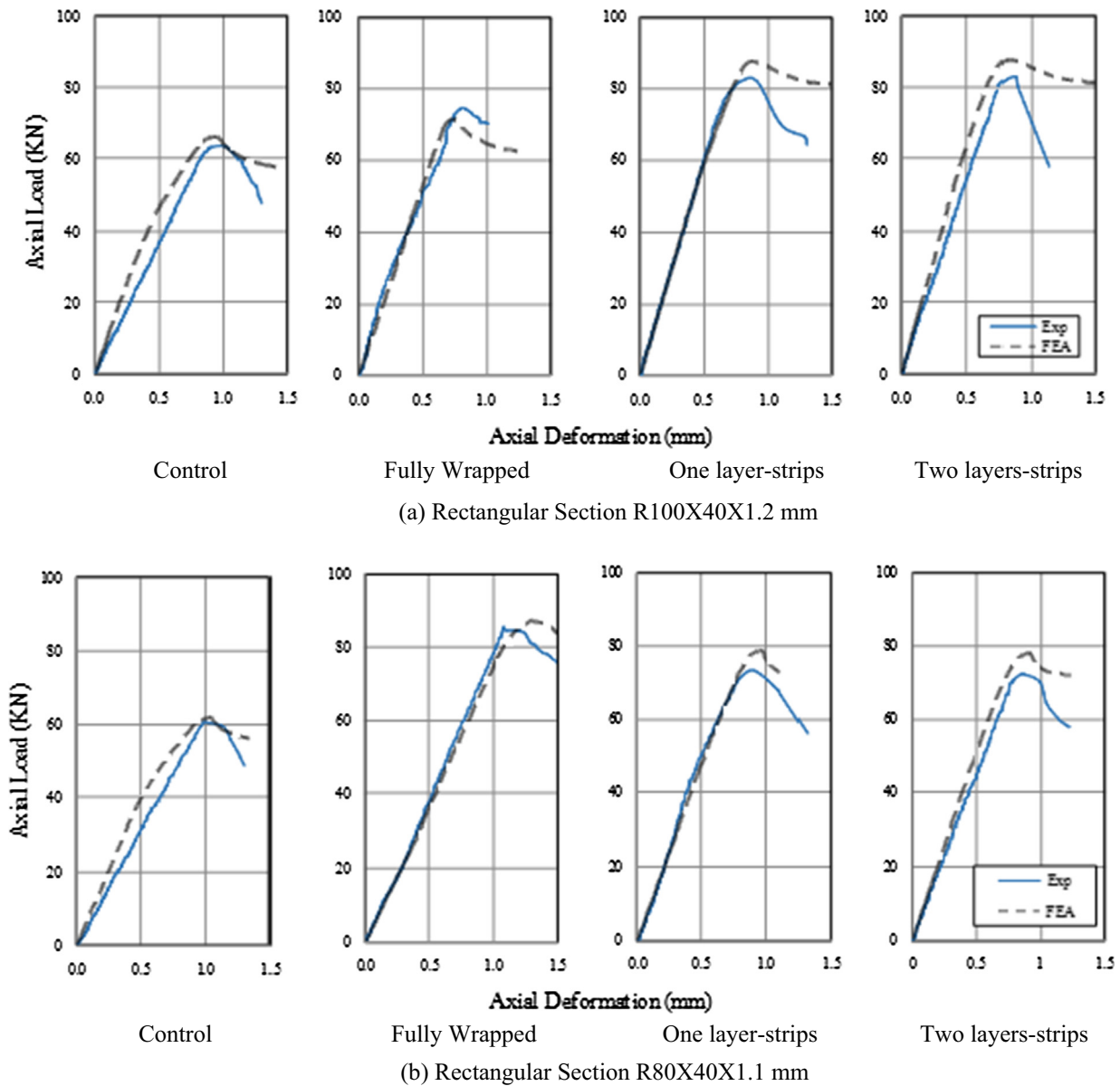


Fig. 14. Comparison between experimental and analytical load-deformation relations, for the studied RHS short columns.

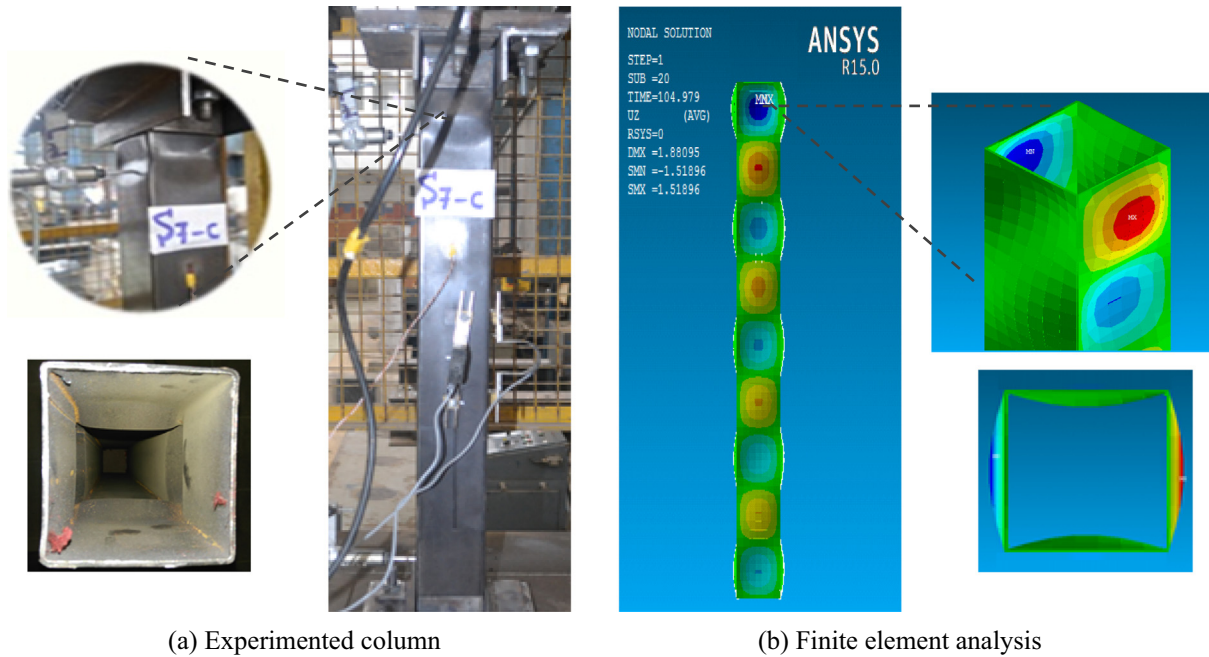


Fig. 15. Post local buckling failure at control column (S7-C).

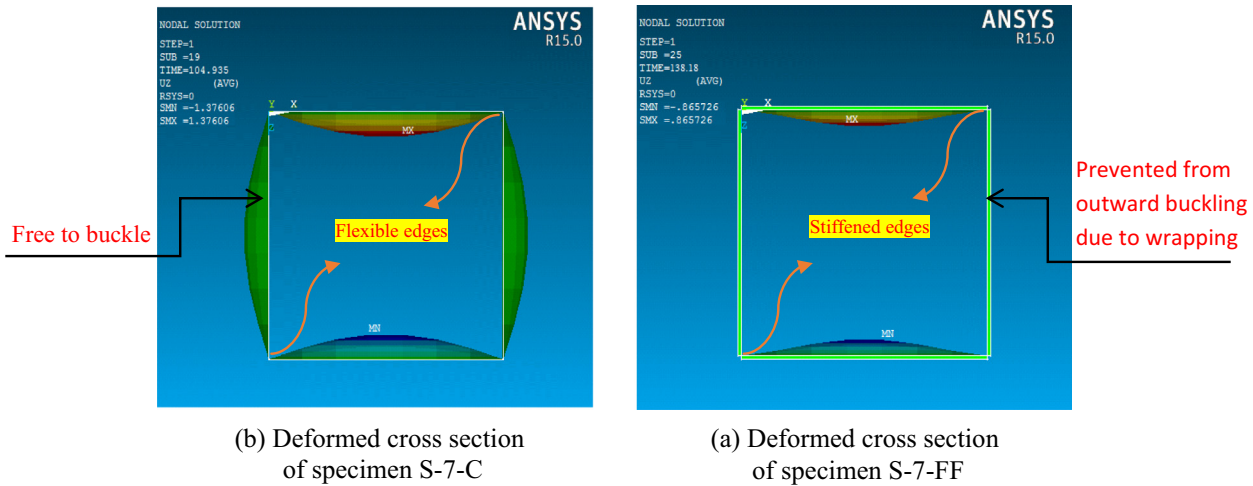


Fig. 16. The lateral deformation at cross section of control and fully wrapped columns of section $S70 \times 70 \times 1.4$.

tion on the long edges for each plate depends on the relative rigidity of the perpendicular adjacent plates. Plate slenderness factor (λ_p) can be estimated by the following equation:

$$\lambda_p = \sqrt{\frac{f_y}{f_{cr}}} \quad (1)$$

where; f_{cr} is the elastic critical buckling stress of the plate. The critical buckling stress of the individual plate can be calculated from the theoretical equation of plate buckling stress developed by Timoshenko and Gere [28]:

$$f_{cr} = \frac{k\pi^2 E}{12(1-\nu^2)} \left(\frac{t}{b}\right)^2 \quad (2)$$

where b is the plate width, t is the plate thickness, ν is the Poisson's ratio and K is the buckling coefficient. The factor K is dependent on

the plate boundary condition. It is equal to 4.0 for simply supported long plates, Timoshenko and Gere [28].

Eq. (2) had been developed for individual plates, however, it can be applied for columns of SHS, as there are no relative rotations at the common edges between the adjacent plates ensuring the simply supported boundary condition along the four edges. This assumption is not applicable in case of RHS, as the relative rigidities of the perpendicular neighboring plates are not equal.

An analytical model based on the analytical equations developed by Badawy Abu Senna A. B. [29] to predict the critical local buckling stress of singly lipped channel section in compression has been developed. The developed model is based on the energy method to predict the most critical local buckling stress and the corresponding critical half wave length for closed hollow sections (RHS or SHS).

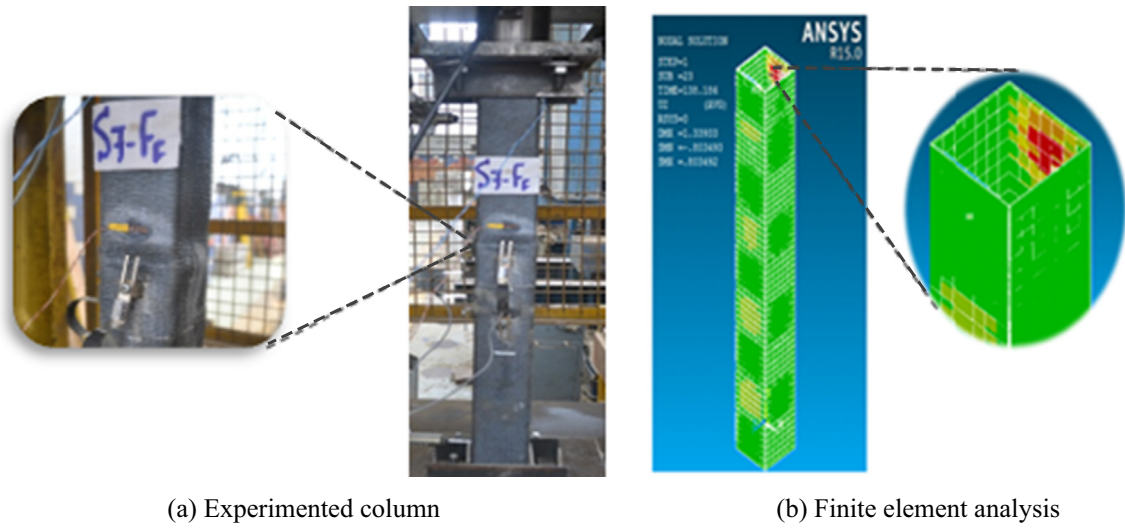


Fig. 17. Failure mode for fully wrapped specimen, representative column S-7-FF.

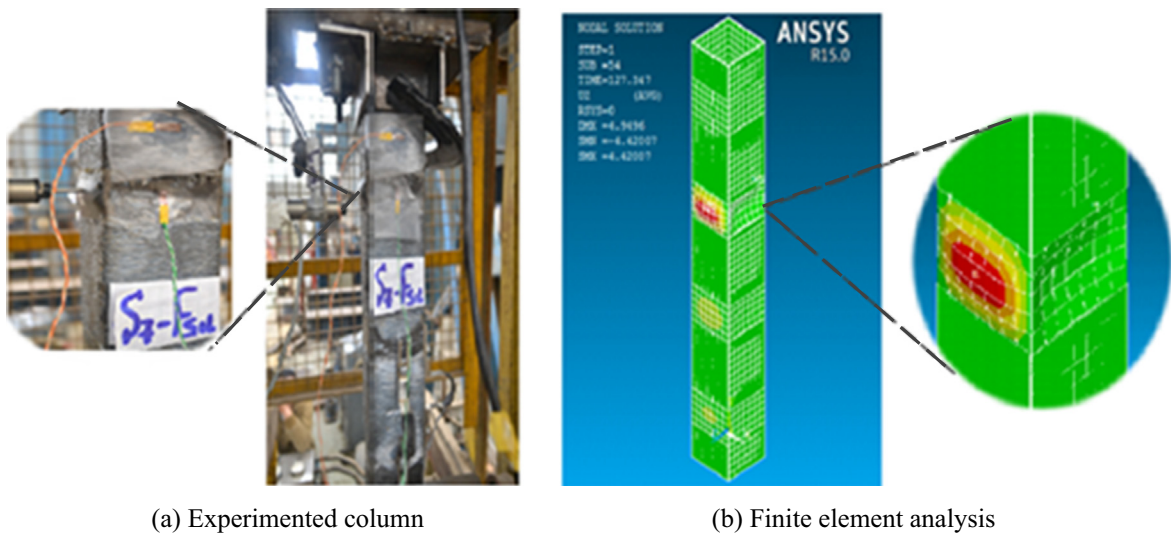


Fig. 18. Failure at partially strengthened column of one layer strips S-7-FS1L.

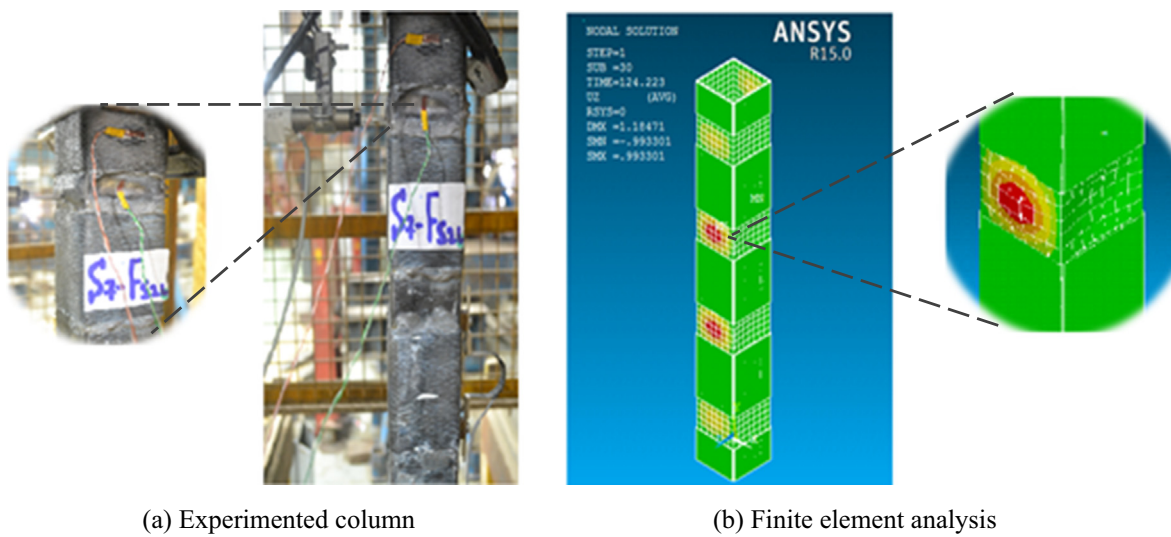


Fig. 19. Failure at partially strengthened column of two layer strips S-7-FS2L.

Table 6
Expressions for the coefficient $K_p(i,j)$ used in Eqs. (3.a) and (3.b).

	$i = 1$	$i = 2$
$j = 1$	$\frac{8}{15} + 2 \left[\frac{2}{\pi} \left(1 + \frac{2D}{3B} \right) \right]^2 - \frac{128}{\pi^4} \left(1 + \frac{2D}{3B} \right)$	$\frac{8}{15} + 2 \left[\frac{2}{\pi} \left(1 + \frac{2B}{3D} \right) \right]^2 - \frac{128}{\pi^4} \left(1 + \frac{2B}{3D} \right)$
$j = 2$	$\frac{8}{3} - \frac{64}{\pi} \left(1 + \frac{2D}{3B} \right) + 4 \left(1 + \frac{2D}{3B} \right)^2$	$\frac{8}{3} - \frac{64}{\pi} \left(1 + \frac{2B}{3D} \right) + 4 \left(1 + \frac{2B}{3D} \right)^2$
$j = 3$	$4 - 8 \left(1 + \frac{2D}{3B} \right) + \frac{\pi^2}{2} \left(1 + \frac{2D}{3B} \right)^2$	$4 - 8 \left(1 + \frac{2B}{3D} \right) + \frac{\pi^2}{2} \left(1 + \frac{2B}{3D} \right)^2$

Eq. (3.a) gives the critical local buckling stress for a rectangular hollow section (RHS). The corresponding critical number of half waves (m_{cr}) is given by Eq. (3.b).

$$f_{cr} = \sum_{i=1}^2 \frac{D_{fi} \left[\left(\frac{m_{cr}\pi}{L} \right)^2 K_{P(i,1)} d_i + \frac{K_{P(i,2)}}{d_i} + \left(\frac{L}{m_{cr}\pi} \right)^2 \frac{K_{P(i,3)}}{d_i^3} \right]}{t_i d_i K_{P(i,1)}} \quad (3.a)$$

$$m_{cr} = \frac{L}{\pi} \sqrt[4]{\sum_{i=1}^2 \frac{K_{P(i,3)}}{d_i^4 K_{P(i,1)}}} \quad (3.b)$$

where:

d_1 : is the half of section width ($B/2$).

d_2 : is the half of section depth ($D/2$).

D_{F1} and D_{F2} : are the flexural rigidity of the two plates, given by:

$$D_{F1} = D_{F2} = \frac{Et^3}{12(1 - \nu^2)} \quad (4)$$

$K_p(i,j)$ ($i = 1, 2$, and $j = 1-3$) are dimensionless coefficients that can be expressed in terms of the section geometry. General expressions for these coefficients are given in Table 6.

Expression (3.b) can be used to calculate the most preferred number of half waves corresponding to the lowest critical buckling given by expression (3.a). The critical half wave length (λ_{cr}) can be alternatively used instead of m_{cr} , as given by Eq. (4).

$$\lambda_{cr} = \frac{L}{m_{cr}} = \pi \sqrt[4]{\sum_{i=1}^2 \frac{d_i^4 K_{P(i,1)}}{K_{P(i,3)}}} \quad (5)$$

For a given column length, m_{cr} is usually a non-integer number, which should be approximated to the closest integer number, and the critical local buckling stress will be the value corresponding to this integer number which is slightly higher than the value corresponding to the non-integer number.

The square hollow section is a special case of the rectangular section so, we can apply equations 3 and 5 for SHS columns with considering that $b = d$. The results obtained from equations 3 and 5 are compared to the finite element Eigen value analysis in Table 7.

6. Parametric study

From the results of analysis presented in the previous sections, it can be noticed that there are two main parameters that affect the percentage of strength enhancement resulting from utilizing the

CFRP strengthening scheme. The first parameter is the individual plate slenderness, and the second is distance between strips. The effect of the two parameters has been studied for both square and rectangular sections using the finite element non-linear analysis. To perform the comparisons; Young’s modulus and yielding strength of steel are considered to be 200 GPa and 350 MPa respectively for all specimens.

Fig. 20a shows the variation of the percentage of enhancement due to full wrapping with the individual plate slenderness ratios for square sections. Fig. 20b. shows the variation of the percentage of enhancement due to full wrapping with the long plate slenderness ratios for rectangular hollow sections.

It can be noticed from the two figures that the percentage of strength increases with increasing the slenderness of plates. For both square and rectangular section failure may occur due to yielding in low slenderness sections; this means wrapping process will not significantly affect the failure load. As the slenderness ratio



Fig. 20a. Variation of strength enhancement percentage with plate slenderness ratio for fully wrapped square hollow section (100 × 100 mm).

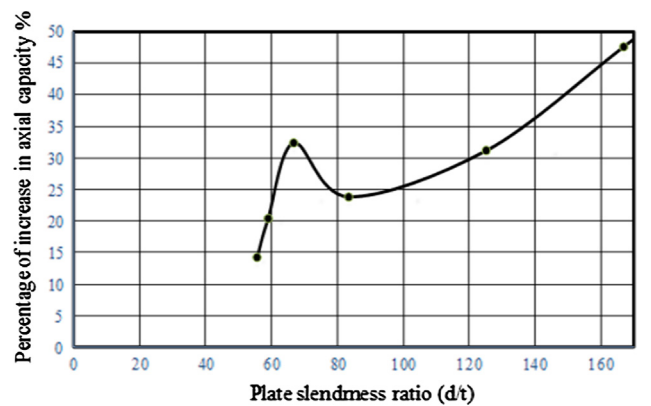


Fig. 20b. Variation of strength enhancement percentage with long plate slenderness ratio for fully wrapped rectangular hollow section (100 × 40).

Table 7
Comparison between the analytical model and finite element Eigen value analysis.

Section	Local buckling stress (Analytical Eq. (3.a)) (MPa)	Local buckling stress by F.E. Eigen value analysis (MPa)	Analytical/Finite Element	Yield stress (MPa)	Critical half wave length λ_{cr} (Eq. (5)) (mm)
S-100 × 100 × 1.5	153.2	150.2	1.02	303.0	100.0
S-80 × 80 × 1.5	231.0	231.7	1.0	456.0	75.0
S-70 × 70 × 1.4	271.7	275.7	0.99	397.0	67.0
R-40 × 100 × 1.2	137.7	133.4	1.03	360.0	75.0
R-40 × 80 × 1.1	178.7	173.6	1.03	385.0	67.0

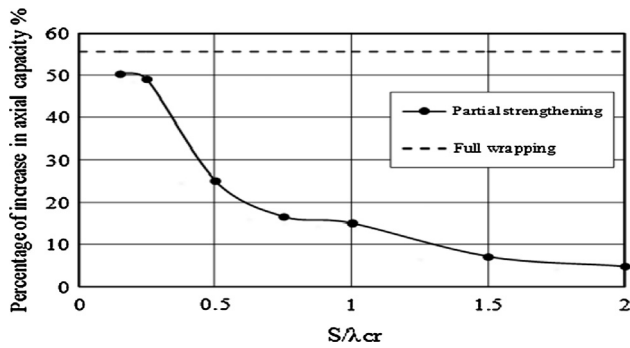


Fig. 21a. Variation of strength enhancement percentage with strips spacing for partially strengthened square hollow section $100 \times 100 \times 1.5$ mm.

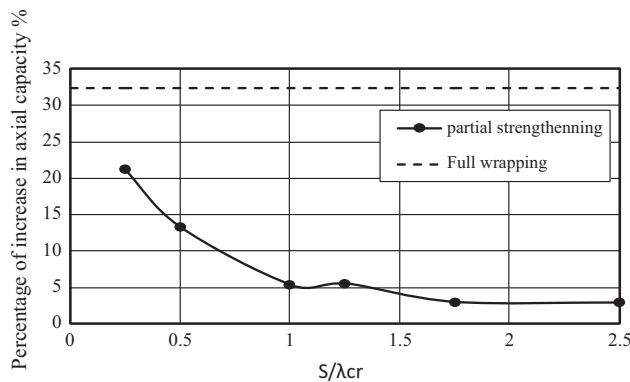


Fig. 21b. Variation of strength enhancement percentage with strips spacing for partially strengthened rectangular hollow section $100 \times 40 \times 1.5$ mm.

increases, the local buckling begins to be the dominate failure that describes the changes in curves slope. It can be also noticed that, strengthening using CFRP wrapping is more efficient in case of square sections than the case of rectangular sections.

In case of partially strengthened SHS and RHS columns, the increase in axial capacity depends on the spacing between the CFRP strips. Fig. 21a. shows the results for a square section $100 \times 100 \times 1.5$, and Fig. 21b. shows the results for a rectangular section $100 \times 40 \times 1.5$. Increasing the spacing between the strengthening strips reduces the enhancement in failure load (Figs. 21a and 21b). Maximum strength enhancement corresponds to minimum strips spacing, however it still smaller than the full wrapping enhancement.

7. Conclusions

An experimental investigation in addition to finite element non-linear analyses have been performed on twenty short SHS and RHS steel columns with different strengthening schemes utilizing CFRP. The experimental results of ultimate capacities of control SHS and RHS specimens were verified with their analytical and numerical counterparts and were found to be in a good agreement with both methods. The external bonding of CFRP sheets by full wrapping technique provides a sufficient confining action against column local deformation, accordingly, delays the elastic local buckling and increases the column axial capacity and stiffness. The enhancement in axial stiffness leads to a noticeable decrease in axial deformation for strengthened columns compared to the control columns. The presence of initial imperfection at RHS may cause the initiation of inward buckling at the larger plate of column that

causes the de-lamination of wrapped CFRP, leading to a premature failure and providing a lower enhancement in axial capacity. The partially strengthening technique delays the elastic buckling occurrence where buckling tends to be formed at the non-strengthened zone between two consecutive strengthened zones. Experimental results showed that, strengthening using strips of two layers has no significant difference than using one layer strips, because the elastic buckling was affected by the width of strips and the interval distance between strips. Numerical results showed that; increasing the local slenderness of the section plates increases the percentage of enhancement in column capacities for fully wrapped columns. However, for partially wrapped columns, the most effective parameter is the distance between the CFRP strips. Increasing the spacing between strips significantly reduces the strength enhancement result from applying the strengthening scheme.

Conflict of interest

None.

References

- [1] W.W. Yu, Cold-formed steel structures, McGraw-Hill, 1973.
- [2] J.L. Dawe, A.A. Elgabry, G.Y. Grondin, Local buckling of hollow structural sections, *ASCE J. Struct. Eng.* 111 (5) (1985) 1101–1112.
- [3] V.M. Karbhari, S.B. Shulley, 'Use of composites for rehabilitation of steel structures, determination of bond durability', *J. Mater. Civ. Eng.* 7 (4) (1995) 239–245.
- [4] T.C. Miller, M.J. Chajes, D.R. Mertz, J.N. Hastings, Strengthening of a steel bridge girder using CFRP plates, *J. Bridge Eng.* 6 (6) (2001) 514–522.
- [5] Zerbo, V., Di Tommaso A. and Ceriolo, L. 2005, "FRP strengthening systems for metallic structures: a state of the art", *Structural Analysis of Historical Constructions - Modena*, Lourenço & Roca (eds), Taylor and Francis Group, London, ISBN 04 15363799, pp 891–900.
- [6] X.-L. Zhao, L. Zhang, State-of-the-art review on FRP strengthened steel structures, *Eng. Struct.* 29 (8) (2007) 1808–1823.
- [7] P. Colombi, C. Poggi, An experimental, analytical and numerical study of the static behavior of steel beams reinforced by pultruded CFRP strips, *Composites Part B: Eng.* 37 (1) (2006) 64–73.
- [8] K. Narmashiri, N.R. Sulong, M.Z. Jumaat, Failure analysis and structural behaviour of CFRP strengthened steel I-beams, *Constr. Build. Mater.* 30 (2012) 1–9.
- [9] E. Ghafoori, M. Motavalli, J. Botsis, A. Herwig, M. Galli, Fatigue strengthening of damaged metallic beams using prestressed unbonded and bonded CFRP plates, *Int. J. Fatigue* 44 (2012) 303–315.
- [10] Q. Yu, T. Chen, X. Gu, X. Zhao, Z. Xiao, Fatigue behaviour of CFRP strengthened steel plates with different degrees of damage, *Thin-Walled Struct.* 69 (2013) 10–17.
- [11] M. Kamruzzaman, M.Z. Jumaat, N. RamliSulong, A. Islam, A review on strengthening steel beams using FRP under fatigue, *Sci. World J.* 2014 (2014) 21. 702537.
- [12] A. Shaat, A. Fam, Axial loading tests on short and long hollow structural steel columns retrofitted using carbon fiber reinforced polymers, *Can. J. Civil Eng.* 33 (4) (2006) 458–470.
- [13] CSA. 2001. Limit states design of steel structures. Standard CAN/CSA S16-01. Canadian Standards Association, Mississauga, Ont.
- [14] M.R. Bambach et al., Axial capacity and design of thin-walled steel SHS strengthened with CFRP, *Thin-Walled Structures* 47 (10) (2009) 1112–1121.
- [15] M.C. Sundararaja et al., Strengthening of hollow square sections under compression using FRP composites, *Adv. Mater. Sci. Eng.* 2014 (2014) 19. 396597.
- [16] M.R. Ghaemdoost, K. Narmashiri, O. Yousefi, Structural behaviors of deficient steel SHS short columns strengthened using CFRP, *Constr. Build. Mater.* 126 (2016) 1002–1011.
- [17] J. Haedir, X.L. Zhao, Design of short CFRP-reinforced steel tubular columns, *J. Constr. Steel Res.* 67 (3) (2011) 497–509.
- [18] M. Sundararaja, B. Shanmugavalli, Experimental investigation on the behaviour CHS short columns strengthened using FRP composites under compression, *Int. J. Adv. Struct. Geotech. Eng.* 3 (2014) 91–97.
- [19] S. NaganathanS. Kalavagunta, K.N.B. Mustapha, Capacity assessment and design of CFRP-strengthened steel channel columns, *Indian J. Sci. Technol.* 6 (4) (2013) 4255–4261.
- [20] British Standard BS5950-5, 1998, "Structural use of steelwork in building", Part 5, Code of practice for design of cold formed thin gauge sections. BSI, UK.
- [21] E.A. Amoush, M.A. Ghanem, Axially loaded capacity of alternatively strengthened cold-formed channel columns with CFRP, *J. Constr. Steel Res.* 140 (2018) 139–152.

- [22] M. Shahraki, M.R. Sohrabi, G. Azizian, K. Narmashiri, Experimental and numerical investigation of strengthened deficient steel SHS columns under axial compressive loads, *Struct. Eng. Mech.* 67 (2) (2018) 207–217.
- [23] M. Karimian, K. Narmashiri, M. Shahraki, O. Yousefi, Structural behaviors of deficient steel CHS short columns strengthened using CFRP, *J. Constr. Steel Res.* 138 (2017) 555–564.
- [24] R. Shahabi, K. Narmashiri, Effects of deficiency location on CFRP strengthening of steel CHS short columns, *Steel Compos. Struct.* 28 (3) (2018) 267–278.
- [25] SIKA EGYPT company, "SikaWrap[®]-300 C. Product data sheet", January 2017, Version 01.01.
- [26] SIKA EGYPT company, "Sikadur[®]-330. Product data sheet", September 2016, Version 01.01.
- [27] E. Pietropaoli, A. Riccio, Finite element analysis of the stability (buckling and post-buckling) of composite laminated structures: well established procedures and challenges, *Appl. Compos. Mater.* 19 (1) (2012) 79–96.
- [28] S.P. Timoshenko J.M. Gere *Theory of Elastic Stability* 1961 McGraw-Hill, New York (Sec 9.2).
- [29] Badawy Abu Senna, A. B., Interaction between local, distortional and overall buckling in open thin walled sections Ph.D. Thesis, Imperial college, London, 1997.